DOI: 10.1002/anie.201005891

Nanostructures

Binary Self-Assembly of Gold Nanowires with Nanospheres and Nanorods**

Ana Sánchez-Iglesias, Marek Grzelczak, Jorge Pérez-Juste, and Luis M. Liz-Marzán**

The assembly of nanoparticles is a crucial step toward their integration within devices. Although self-assembly has been widely studied, directing self-assembly into well-defined orientations is still a major challenge.[1] This is particularly interesting when assembling anisometric nanoparticles, such as rods or wires, because of their anisotropic properties. For example, gold nanorods display orientation-dependent optical response, because excitation of different localized surface plasmon resonance modes occurs as a function of their orientation.[2] In nanorod-pair systems it has been found that interparticle distance and mutual orientation strongly affect the overall optical response.[3,4] Therefore, aligned nanorod assemblies provide notably more interesting properties than their corresponding random assemblies, but implementation of nanoparticle assemblies into devices requires novel methods to achieve controlled organization over large (cm) areas.

The use of templates has been demonstrated as a useful way to direct nanoparticle assembly. For example, gold nanorods were shown to align along carbon nanotube templates,[5] which was explained by enhanced van der Waals interactions. Although this process works in solution, it is difficult to implement on surfaces and it requires multiple surface modification steps. Recent progress on evaporation-driven self-assembly of binary systems[6] points toward cooperative effects when different types of nanocrystals (varying in size, shape, or composition)[7] simultaneously self-assemble on a substrate, so that completely new ordered structures can be achieved. However, binary self-assembly of components with different sizes and aspect ratios (e.g. spheres, rods, wires) can lead to an interesting scenario, in which one kind of particles induces the spatial distribution of the other.[8] Thus, novel structures with geometrical diversity can be obtained over extended length scales. We present herein novel binary systems, in which highly anisotropic gold nanowires drive the oriented assembly of spherical and rod-like gold nanoparticles into extended ordered arrays.

Gold nanospheres[9] (12.8 ± 0.8 nm in diameter), nanorods[10] (length: 37.7 ± 2.3 nm; width: 11.6 ± 0.7 nm), and nanowires[11] (diameter: 1.6 ± 0.2 nm; length > 5 μm) were prepared as previously reported (see representative images in Figure 1). For gold nanowires (AuNWs) and nanospheres (AuNSs), the as-prepared nanoparticles were washed with methanol to ensure elimination of excess oleylamine (OA). Prior to the assembly, the particles were redispersed in hexane at a concentration of 3 mM in gold atoms. Transfer of gold nanorods (AuNRs) from aqueous to organic solvents required applying a ligand-exchange procedure in which the cationic surfactant (cetyltrimethylammonium bromide; CTAB) was first displaced by dodecanethiol (DDT)[12] and the DDT-capped AuNRs were then soaked in a concentrated solution of oleylamine, washed, and redispersed in THF at a concentration of 3 mM (see Experimental Section for details). Optical characterization of the stock solutions confirmed the colloidal stability of all individual nanoparticles, as indicated by the absence of band broadening, which would be an indication of plasmon coupling (Figure S1 in the Supporting Information).

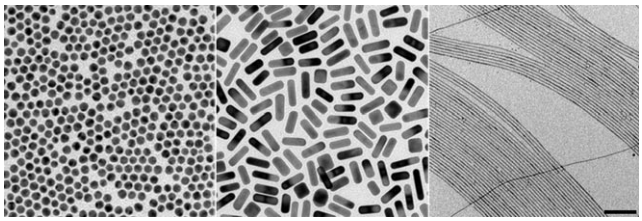

Figure 1. Representative TEM images of gold spheres, rods, and wires used as building blocks for the formation of binary assemblies upon solvent evaporation. Scale bar: 50 nm.

Binary self-assembly was initially carried out by drop-casting and controlled evaporation on solid substrates, such as glass or carbon-coated TEM grids.[7,8] However, we also explored a recently reported method for interfacial self-assembly of nanocrystals,[13] in which nanoparticles were organized from a dispersion in hexane, through rapid evaporation on a liquid diethyleneglycol (DEG) subphase. Typically, a hexane solution containing the mixture of AuNWs and either spheres or rods was deposited on the selected substrate, and the droplet was allowed to evaporate under ambient conditions (10 s–10 min), leading to a change of the initial red color into purple/blue upon complete solvent evaporation (see Supporting Information video).

[*] A. Sánchez-Iglesias, Dr. J. Pérez-Juste, Prof. L. M. Liz-Marzán
Departamento de Quimica Fisica and Unidad Asociada CSIC
Universidade de Vigo, 36310 Vigo (Spain)
Fax: (+34) 986-812-556
E-mail: lmarzan@uvigo.es
Dr. M. Grzelczak
Dipartimento di Scienze Farmaceutiche
Università degli Studi di Trieste, 34127 Trieste (Italy)
E-mail: grzelczak.marek@gmail.com

[**] We thank Isobel Pastoriza-Santos for helpful discussions. A.S.-I. acknowledges the Isabel Barreto Program (Xunta de Galicia, Spain). This work has been funded by MiCInn/FEDER (MAT2007-62696), Xunta de Galicia (09TMT011314PR), and by the EU (NANODIRECT, grant number CP-FP 213948-2).

Supporting information for this article is available on the WWW under http://dx.doi.org/10.1002/anie.201005891.

As shown in Figure 2, the organization of both spheres and rods in the presence of NWs largely differs from that formed from their respective homogeneous solutions (Figure 1). AuNSs and AuNRs are efficiently incorporated within AuNW bundles formed upon drying,[14] which trap the small particles in a very efficient manner.

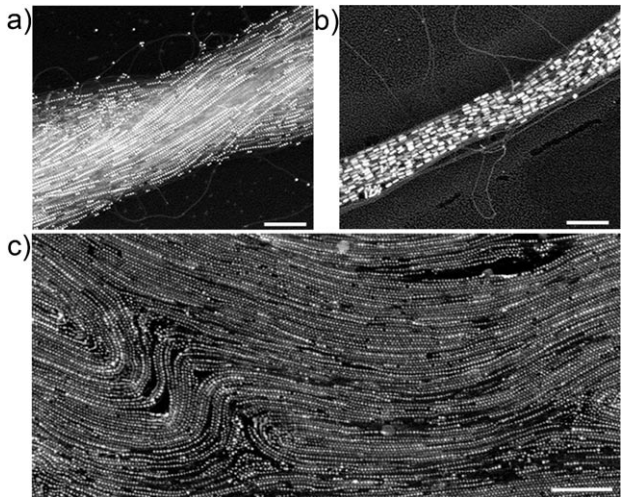

Figure 2. SEM images of gold spheres (a) and rods (b), embedded in AuNW bundles, upon drying on a solid substrate. c) Arrays of nanospheres induced by flexible AuNWs, obtained by self-assembly on a liquid subphase (DEG). Scale bars: 200 nm.

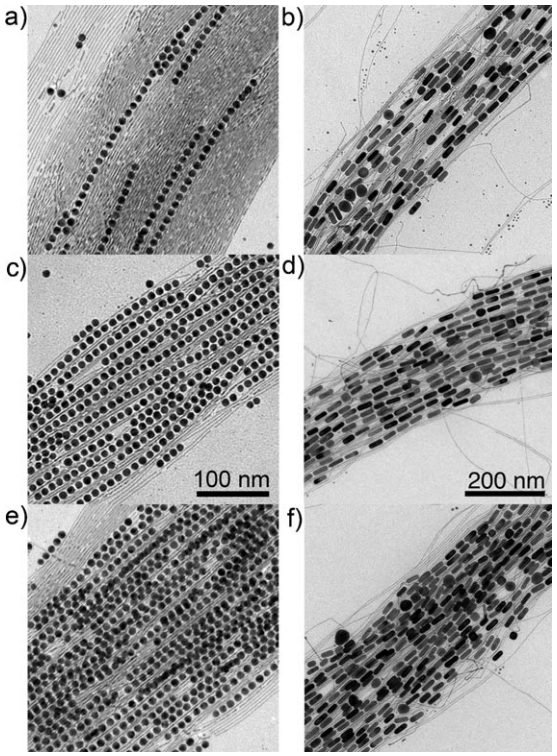

Figure 3. TEM images of binary assemblies containing different amounts of spheres (a,c,e) and rods (b,d,f), at constant nanowire concentration. Increased nanoparticle loading was obtained by increasing the concentration ratio between spheres/rods and wires.

The incorporation of small particles between AuNWs was found to be independent of the nature of the substrate, but the final morphology of the assemblies, in particular for spheres, does rely on the specific substrate used. High-aspect ratio bundles containing nanoparticles between the wires were mostly obtained on solid substrates (Figure 2a,b), while self-assembly on a liquid subphase generally resulted in extended monolayers (ca. 1 cm^2, Figure 2c). This behavior can be related to the low polarity of DEG and its miscibility with oleylamine, which can facilitate the diffusion of the particles into the subphase.[15] The oriented templating character of the nanowires during the assembly is particularly visible in the case of AuNRs, which get organized into aligned stripes (regardless of the substrate), with tip-to-tip mutual orientations, and parallel to the long axis of the AuNWs over several micrometers (Figure 2b and S2).

The binary nature of the assemblies determines that the density of the assembled particles within AuNW bundles can be controlled through the relative nanoparticle concentration in solution. This was demonstrated by varying the amount of spheres/rods (from 0.025 mM to 0.25 mM) at constant nanowire concentration (0.15 mM), which resulted in an increased loading density, as shown in Figure 3. We found that droplet formation (on solid substrates), solvent properties, and the chemical nature of the capping agent are all very important for successful growth of binary assemblies. Both drop-casting the colloidal mixture onto a TEM grid supported on filter paper, and dipping the grid in the colloid, resulted in random distribution of the particles (Figure S3). Additionally, if toluene rather than low-boiling point solvents (pentane, hexane, heptane) was used, separate distributions of small particles and wires were obtained (Figure S4). Similar observations were reported by Murray and co-workers for their binary assemblies on liquid substrates.[13] Finally, we also found that the presence of a certain excess of oleylamine in solution was needed to achieve the assembly, in particular for the NRs/NWs system. The assembly of AuNRs required sequential ligand exchange, involving CTAB replacement with thiolated polyethylene glycol (PEG)[16] and PEG replacement with DDT[12] (Experimental Section). Binary assembly was attempted using AuNRs@PEG and AuNRs@DDT, for various concentrations of OA in solution. PEG-capped AuNRs failed to assemble in the presence of AuNWs (Figure S5a,b), even with excess oleylamine, suggesting that the long polymer (PEG) sterically hinders the adsorption of the short aliphatic chains from OA on the nanowires. However, incorporation of an alkanethiol (DDT) on the gold nanorods surface by (partial) PEG removal,[17] allowed binary assembly, but only with OA present in solution (Figure S5c). Although the amine groups from oleylamine have lower affinity to gold than the thiol groups from DDT or PEG, these observations are in agreement with earlier reports regarding the importance of free excess ligand (mainly thiols) toward binary system formation.[18–20] We hypothesize that the similar length of DDT and OA aliphatic chains allow interdigitation, thereby stabilizing the binary assemblies.[21,22] O'Brien and co-workers suggested that such ligands (organic

polar molecules) act as high boiling point solvents, capable of confining nanoparticles into slowly evaporating droplets, thereby elongating the time needed for crystal formation.[18] In addition, Prasad et al. claimed that during crystal formation, free molecules get "excluded" as the particles come together and then trapped at interstitial sites within the superlattices.[20] This in turn is related to the observation by Manna and co-workers[21] that addition of OA to a dispersion of semiconductor nanorods resulted in side-to-side interactions driven by depletion forces. In sum, besides the complexity derived from the non-equilibrium nature of evaporative self-assembly, these systems add additional intricacy because of extreme deviation from the spherical shape of one of the components. We thus expect a complex balance between different driving forces such as core–core and ligand–ligand van der Waals forces[23] or even depletion forces.[21]

Generally, self-assembly on solid substrates is driven by capillary flow in the drying droplets, due to compensation of the rapid solvent evaporation at the contact line, by outward flow from the central part toward the perimeter of the drop.[24] This flow can direct the nanoparticles toward the edges, where they get accumulated/assembled. In our case, the solvent (hexane, ca. 10 μL) evaporates within a few seconds, thus minimizing the time allowed for particles to flow toward the edges. We propose that the distribution of the binary system over the entire surface of the dried droplet is nearly homogeneous (which is reflected in a uniform coloration of the films),[25] and that intercalation of the small particles between the wires in the fast evaporating mixture is driven by entropy.[7,23] In addition, the nucleation of binary crystals in this process is likely to occur simultaneously at multiple sites during drying, which would explain the preferential formation of bundles rather than a perfectly uniform monolayer.

On the other hand, self-assembly on a liquid subphase leads to the formation of extended monolayers, in accordance with an assembly mechanism driven by convective flow.[26] In this process, the height of the colloidal suspension (hexane, ca. 1 mL) covering the liquid substrate is always thinner at the center of the well and gradually becomes thicker with radial distance, toward the periphery of the well (see Supporting Information movie). Thus, the concave hexane droplet evaporates faster in the middle, leading to an inward flow that carries the particles toward the growing monolayer. Again, we expect the particles intercalation between NWs to be an entropy-driven process. The main advantages of carrying out the self-assembly from the concave droplet on the liquid substrate arise from the following issues: 1) the "dynamic" subphase can adapt itself to the above-formed superlattice; 2) diffusion of particles along the interface is facilitated by miscibility of the capping agent (OA) with the liquid subphase; 3) solvent evaporation rate permits a better control over feeding of ordered domains with new particles.

The optical properties of the binary assemblies were analyzed for samples prepared at liquid interfaces, because of the better quality and extension of these systems (Figure 4). We thus transferred assembled nanoparticles from the liquid to a glass substrate by means of the Langmuir–Schaefer technique,[26] that is, by simply touching the hydrophobic surface containing the nanoparticles with a glass slide and lifting it from the subphase (Figure 4). We first investigated the NW–NS binary system, for which the plasmon band mostly originates from the spheres, because the ultrathin wires display no plasmon resonance in the visible region.[14] It should be noted that the interparticle spacing between AuNSs parallel to the long axis of the AuNWs is smaller (1.5 ± 0.4 nm) than that in the perpendicular direction (5.2 ± 1.0 nm; Figures 3 and 4). These small interparticle distances promote strong plasmon coupling and therefore red-shift of the plasmon band.[27] However, the dielectric constant near the particles is also increased due to the presence of the AuNWs, which could also contribute to the red-shift. The AuNS plasmon band, initially located at 523 nm (Figure 4a, spectrum 1), was red-shifted by 50 nm upon binary assembly (Figure 4a, spectrum 3). This plasmon shift is in agreement with reported results for 2D superlattices made from DNA-capped gold nanoparticles, also featuring dissimilar interparticle distances in different directions.[28] Stronger optical changes were observed in hexagonal superlattices arising from self-assembly of the AuNSs alone, in which the interparticle distance was equally short in all directions (1.5 ± 0.4 nm; Figure 4). The plasmon band was then red-shifted by 115 nm (Figure 4a, spectrum 2), in agreement with literature values.[29] These observations confirm the well-known result that small changes in the separation between AuNSs drastically affect their collective optical response, in such a way that it can even be detected by the naked eye.

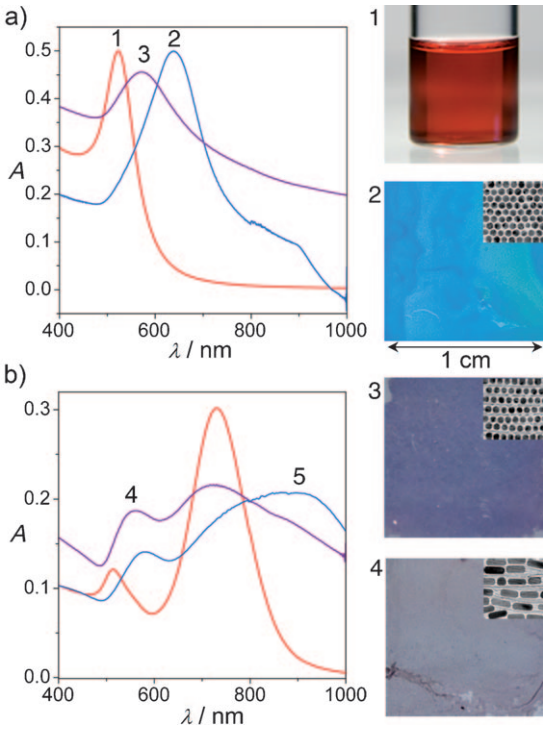

Figure 4. Vis/NIR spectra of assembled gold nanospheres (a) and nanorods (b) on a liquid subphase, using nanowires as templates. Spectra 2 and 5 correspond to assemblies made from spheres and rods alone, respectively. The right panel shows digital photographs and corresponding representative TEM micrographs of nanoparticle assemblies transferred onto glass slides, demonstrating the various colors for the different assemblies, as well as for a solution of spheres.

When gold nanorods were assembled within AuNWs, both the transverse and longitudinal plasmon bands became notably broadened, again due to plasmon coupling (Figure 4b, spectrum 4). Whereas the transverse plasmon band (TPB) was red-shifted by 47 nm, the maximum of the longitudinal plasmon band (LPB) remained apparently unchanged but the band was significantly broadened. It has been shown that in the AuNR-pair system, side-to-side interactions lead to a red-shift of the TPB and blue-shift of the LPB, while tip-to-tip arrangements would red-shift both bands.[3,30] In our multiparticle system, although the AuNRs tend to form oriented arrays, many different mutual orientations and separations are possible, the result being partial cancellation of the plasmon shifts and broadening because of the wide variety of "coupled resonances". Pure AuNR monolayers also showed larger optical changes (Figure 4b, spectrum 5). The TPB red-shifted 65 nm, while LPB shifted 150 nm, both with significant broadening, because of strong plasmon coupling at smaller interparticle distances (3.3 ± 0.7 nm side-to-side, Figure S6), as compared to those in the binary system (6.5 ± 1.9 nm). As expected, the gaps in tip-to-tip direction were found to be essentially equal for both assemblies (3.4 ± 0.7 nm).[31]

In conclusion, we have shown that gold nanowires can induce the assembly of nanospheres and nanorods into ordered arrays when oleylamine is present on their surfaces and in solution. Moreover, nanowires can tune distances between nanoparticles, thereby altering the overall optical response of the film, as observed by naked eye. These examples raise new promises in bottom-up fabrication, especially for sensing or optoelectronic devices, where controlled interparticle separation is required. Future prospects envisage the use of magnetic or semiconductor nanocrystals, with the possibility of tuning their optical or magnetic response. Additionally, the thermal instability of the templating nanoparticles allows post-synthetic transformations, as a response to external stimuli (Supporting Information, Figure S7).

Experimental Section

Nanocrystal synthesis: AuNWs and AuNSs were synthesized according to procedures described in the literature.[9,11] Particles were washed in methanol and redispersed in hexane ([Au] = 3 mM). AuNRs were prepared by seeded growth.[10] Dispersion of AuNRs in organic solvents required stepwise surface functionalization. As-prepared AuNRs (30 mL; [CTAB] = 0.1 M; [Au] = 0.5 mM) were centrifuged (8000 rpm, 40 min) and redispersed in 30 mL of 0.015 M CTAB solution, followed by centrifugation and redispersion in 25 mL of water. To this mixture, 5 mL aqueous PEG-SH solution (20 molecules nm^{-2} of particles) was added drop-wise under vigorous stirring. The solution was then washed twice by centrifugation (8000 rpm, 40 min) and redispersed in 5 mL ethanol. The AuNRs@PEG solution (5 mL) was added drop-wise to 5 mL THF, containing DDT (400 molecules nm^{-2} of particles) and the mixture was sonicated for 1 h and incubated overnight, followed by twofold washing and redispersion in 5 mL THF. Subsequently, 5 mL of OA solution (4 mL of THF and 1 mL of 80% OA) was added drop-wise under sonication to 5 mL of AuNRs@DDT (THF). After 1 h sonication and overnight incubation, they were centrifuged and redispersed in THF ([Au] = 3 mM). Prior to self-assembly, the particles binary mixtures (2 mL) were prepared containing AuNWs (0.15 mM) and AuNSs/AuNRs with appropriate concentrations (0.025 mM, 0.1 mM, or 0.25 mM).

Self-assembly: Binary assembly on solid substrates (carbon-coated nickel TEM grids supported on glass) was obtained by drop-casting 10 μL of the binary mixture. In the course of 10 s the droplet was totally dried. To prepare binary assemblies on liquid substrates, 1 mL of the binary mixture was spread on the DEG surface inside a Teflon well. The well was covered with a glass slide and hexane was allowed to evaporate (ca. 10 min). To transfer the binary systems, the superlattice film on the DEG surface was lightly touched by the solid substrate (carbon-coated nickel TEM grid or glass slide) and gently lifted. The substrates were dried on filter paper.

Instrumentation: Optical characterization was carried out by UV/Vis/NIR spectroscopy with a Cary 5000 spectrophotometer. TEM images were obtained with a JEOL JEM 1010 transmission electron microscope operating at an acceleration voltage of 100 kV. SEM images were obtained using a JEOL JSM-6700F FEG microscope operating at 3.0 kV for secondary electron imaging (SEI).

Received: September 20, 2010
Published online: November 16, 2010

Keywords: binary assembly · gold nanoparticles · nanorods · nanowires · self-assembly

[1] M. Grzelczak, J. Vermant, E. M. Furst, L. M. Liz-Marzán, *ACS Nano* **2010**, *4*, 3591 – 3605.
[2] J. Pérez-Juste, B. Rodríguez-González, P. Mulvaney, L. M. Liz-Marzán, *Adv. Funct. Mater.* **2005**, *15*, 1065 – 1071.
[3] A. M. Funston, C. Novo, T. J. Davis, P. Mulvaney, *Nano Lett.* **2009**, *9*, 1651 – 1658.
[4] L. S. Slaughter, Y. Wu, B. A. Willingham, P. Nordlander, S. Link, *ACS Nano* **2010**, *4*, 4657 – 4666.
[5] M. A. Correa-Duarte, J. Pérez-Juste, A. Sánchez-Iglesias, M. Giersig, L. M. Liz-Marzán, *Angew. Chem.* **2005**, *117*, 4449 – 4452; *Angew. Chem. Int. Ed.* **2005**, *44*, 4375 – 4378.
[6] D. V. Talapin, J. Lee, M. V. Kovalenko, E. V. Shevchenko, *Chem. Rev.* **2010**, *110*, 389 – 458.
[7] E. V. Shevchenko, D. V. Talapin, N. A. Kotov, S. O'Brien, C. B. Murray, *Nature* **2006**, *439*, 55 – 59.
[8] T. Ming, X. Kou, H. Chen, T. Wang, H. Tam, K. Cheah, J. Chen, J. Wang, *Angew. Chem.* **2008**, *120*, 9831 – 9836; *Angew. Chem. Int. Ed.* **2008**, *47*, 9685 – 9690.
[9] H. Hiramatsu, F. E. Osterloh, *Chem. Mater.* **2004**, *16*, 2509 – 2511.
[10] B. Nikoobakht, M. A. El-Sayed, *Chem. Mater.* **2003**, *15*, 1957 – 1962.
[11] H. Feng, Y. Yang, Y. You, G. Li, J. Guo, T. Yu, Z. Shen, T. Wu, B. Xing, *Chem. Commun.* **2009**, 1984 – 1986.
[12] B. Thierry, J. Ng, T. Krieg, H. J. Griesser, *Chem. Commun.* **2009**, 1724 – 1726.
[13] A. Dong, J. Chen, P. M. Vora, J. M. Kikkawa, C. B. Murray, *Nature* **2010**, *466*, 474 – 477.
[14] N. Pazos-Pérez, D. Baranov, S. Irsen, M. Hilgendorff, L. M. Liz-Marzán, M. Giersig, *Langmuir* **2008**, *24*, 9855 – 9860.
[15] V. Aleksandrovic, D. Greshnykh, I. Randjelovic, A. Frömsdorf, A. Kornowski, S. V. Roth, C. Klinke, H. Weller, *ACS Nano* **2008**, *2*, 1123 – 1130.
[16] C. Fernández-López, C. Mateo-Mateo, R. A. Alvarez-Puebla, J. Pérez-Juste, I. Pastoriza-Santos, L. M. Liz-Marzán, *Langmuir* **2009**, *25*, 13894 – 13899.
[17] Direct CTAB displacement with DDT led to irreversible aggregation of particles, thus introduction of an intermediate PEG layer provides steric stabilization of AuNRs upon ligand exchange process (see Ref. [12]).
[18] C. Lu, Z. Chen, S. O'Brien, *Chem. Mater.* **2008**, *20*, 3594 – 3600.

[19] T. P. Bigioni, X. Lin, T. T. Nguyen, E. I. Corwin, T. A. Witten, H. M. Jaeger, *Nat. Mater.* **2006**, *5*, 265 – 270.
[20] D. S. Sidhaye, B. L. V. Prasad, *Chem. Mater.* **2010**, *22*, 1680 – 1685.
[21] D. Baranov, A. Fiore, M. van Huis, C. Giannini, A. Falqui, U. Lafont, H. Zandbergen, M. Zanella, R. Cingolani, L. Manna, *Nano Lett.* **2010**, *10*, 743 – 749.
[22] A. Guerrero-Martínez, J. Pérez-Juste, E. Carbó-Argibay, G. Tardajos, L. M. Liz-Marzán, *Angew. Chem.* **2009**, *121*, 9648 – 9652; *Angew. Chem. Int. Ed.* **2009**, *48*, 9484 – 9488.
[23] Z. Chen, J. Moore, G. Radtke, H. Sirringhaus, S. O'Brien, *J. Am. Chem. Soc.* **2007**, *129*, 15702 – 15709.
[24] R. D. Deegan, O. Bakajin, T. F. Dupont, G. Huber, S. R. Nagel, T. A. Witten, *Nature* **1997**, *389*, 827 – 829.
[25] Different spectra were taken in different areas of each substrate showing identical position of the plasmon bands.
[26] V. Santhanam, J. Liu, R. Agarwal, R. P. Andres, *Langmuir* **2003**, *19*, 7881 – 7887.
[27] S. K. Ghosh, T. Pal, *Chem. Rev.* **2007**, *107*, 4797 – 4862.
[28] W. Cheng, M. J. Campolongo, J. J. Cha, S. J. Tan, C. C. Umbach, D. A. Muller, D. Luo, *Nat. Mater.* **2009**, *8*, 519 – 525.
[29] H. Yockell-Lelièvre, D. Gingras, R. Valle'e, A. M. Ritcey, *J. Phys. Chem. C* **2009**, *113*, 21 293 – 21 302.
[30] P. K. Jain, S. Eustis, M. A. El-Sayed, *J. Phys. Chem. B* **2006**, *110*, 18243 – 18253.
[31] S. Vial, I. Pastoriza-Santos, J. Pérez-Juste, L. M. Liz-Marzán, *Langmuir* **2007**, *23*, 4606 – 4611.

